Journal of Solid State Chemistry 184 (2011) 1208–1215

Contents lists available at ScienceDirect

Journal of Solid State Chemistry

journal homepage: www.elsevier.com/locate/jssc

Periodic mesoporous organosilicas with co-existence of diurea and sulfanilamide as an effective drug delivery carrier

Surendran Parambadath, Vijay Kumar Rana, Santha Moorthy, Sang-Wook Chu, Shin-Kyu Park, Daewoo Lee, Giju Sung, Chang-Sik Ha *

Department of Polymer Science and Engineering, Pusan National University, Geumjeong-gu, Busan 609-735, Republic of Korea

ARTICLE INFO

Article history:
Received 12 November 2010
Received in revised form
9 February 2011
Accepted 2 March 2011
Available online 21 March 2011

Keywords:
Periodic mesoporous organosilica (PMO)
Organic–inorganic hybrid materials
Diurea sulfanilamide
Drug delivery
Drug release

ABSTRACT

In this article we report the synthesis of new periodic mesoporous organosilicas (PMOs) with the co-existence of diurea and sulfanilamide-bridged organosilica that are potentially useful for controlled drug release system. The materials possess hexagonal pores with a high degree of uniformity and show long-range order as confirmed by the measurements of small-angle X-ray scattering (SAXS), N_2 adsorption isotherms, and transmission electron microscopy(TEM). FT-IR and solid state ^{29}Si MAS and ^{13}C CP MAS NMR spectroscopic analyses proved that the bridging groups in the framework are not cleaved and covalently attached in the walls of the PMOs. It was found that the organic functionality could be introduced in a maximum of 10 mol% with respect to the total silicon content and be thermally stable up to 230 °C. The synthesized materials were shown to be particularly suitable for adsorption and desorption of hydrophilic/hydrophobic drugs from a phosphate buffer solution at pH 7.4.

1. Introduction

Periodic mesoporous organosilicas (PMOs) are considered as derivative materials of mesoporous silica, which can be obtained by condensation of organo-bridged silsesquioxane precursors in the presence of organic soft templates [1]. These materials have attracted increasing research attention in materials science because of their homogeneous distribution of organic groups inside the framework, high loading of organic groups, large surface areas (up to 1000 $m^2 g^{-1}$) and pore volumes (1 $cm^3 g^{-1}$) [2]. In addition, varying the processing parameters allows for the production of materials with different appearances, such as films, powders, or monoliths. Reactions with organic groups permit the functionalization of the pore walls and therefore the chemical properties of the materials [3]. However, due to the rigidity prerequisite for the bridging groups and limited availability of the bridged silane precursors, most of the organic bridging groups in the existing PMOs are chemically inert. The chemical inertness of the typical bridging groups widely used in PMOs offers few possibilities for further chemical modification, greatly limiting their application. By choosing the appropriate linker molecules it is also possible to synthesize PMO materials that exhibit various new and interesting properties, which is unknown in pure siliceous mesostructured materials. Co-condensation has been widely employed to introduce different types of organic groups with specific functionality into ordered mesoporous silica materials. The high loading rate and uniform dispersion of organic moieties in the framework, as well as various surface properties imparted from different functional groups endow the PMO materials for various types of applications such as catalysis, ion exchange, encapsulation of transition metal complexes, chemical sensing, nano-material fabrications, and adsorption of metal ions and drugs [4–8].

During the past three decades, controllable drug release system which can deliver the therapeutic drugs to the targeted cells or tissues in a controlled manner and enhanced drug efficiency with reduced toxicity has attracted much attention. So far, a large variety of materials, such as biodegradable polymers [9], hydroxyapatite [10], calcium phosphate cement [11], hydrogels [12], and mesoporous silica have been employed in controlled drug delivery systems [13–15]. Among these drug delivery carriers, ordered mesoporous silica (MS) materials are of special interest due to their stable mesoporous structure, uniform and tunable pore size, high pore volume, large surface area, nontoxic nature, easily modified surface properties, and good biocompatibility. Recently urea bridged PMO materials offer a good candidature in the adsorption of metal ions and controlled drug delivery applications due to its hydrophilic property and ease of synthesis [16–22]. There has been an ever increasing interest in developing effective drug delivery systems (DDS), largely driven by the need to improve effectiveness in controlling the release rate. It is well recognized that an efficient

* Corresponding author. Fax: +82 51 514 4331.
E-mail address: csha@pnu.edu (C.-S. Ha).

0022-4596/$ - see front matter © 2011 Elsevier Inc. All rights reserved.
doi:10.1016/j.jssc.2011.03.003

delivery system should have the capability to transport the desired guest molecules without any loss before reaching the targeted location. Upon reaching the destination, the system needs to be able to release the cargo in a controlled manner. Fabricating a suitable material as carrier is one of the critical factor in controlling the storage volume and release rate of a drug. Any premature release of guest molecules poses a challenging problem. The drug is usually deposited on the active site of the carrier materials by means of Van der waal's force of interaction, hydrophilic–hydrophilic or hydrophobic–hydrophobic interaction [23–34]. In brief, periodic mesoporous silicas (PMS), such as MCM-41 and SBA-15, have been widely investigated as potential drug carriers [25–34], where ibuprofen, itraconazole, gentamycin, cis-platinum, aspirin, captopril, and 5-fluorouracil were used as model drugs to study the adsorption and delivery processes. It is obviously advantageous, when using the PMSs having organo-functionality for drug delivery applications over conventional PMS materials. Particularly, sulfanilamide is the starting material for several groups of drugs [35]. The original antibacterial sulfonamides (sometimes called simply sulfa drugs) are synthetic antimicrobial agents that contain the sulfonamide group. On emphasizing this point the synthesis of PMO having sulfanilamide functionality in its wall structure should be a promising candidate as a host for drug delivery application.

Here, we report the potential application of PMO materials with bridging group having sulfonamide and urea functionalities in the same molecule as effective drug carriers. Sulfanilamide molecule was selected for modification by silane coupling reagent to form the precursor. As is known, the amine functionality can easily be coupled with isocyanato functionality at ambient conditions. The synthesized *N*,*N*′-diureylene sulfanilamide (BSDU) bridged periodic mesoporous hybrid material (SDPMOs), in which the bridging group was uniformly distributed in the framework of PMO material by co-condensation of tetraethyl orthosilicate (TEOS) and BSDU using the Pluronic P123 surfactant as template. We have used the materials for the adsorption and desorption of drugs such as captopril and 5-Flurouracil at pH 7.4 to examine the effectiveness of SDPMOs as a drug delivery system.

2. Experimental section

2.1. Materials and reagents

Poly (ethylene oxide)-*b*-poly (propylene oxide)-*b*-poly (ethylene oxide) [$EO_{20}PO_{70}EO_{20}$, Pluronic P123, M_w=5800], 3-(triethoxysilyl) propylisocyanate (IPTES, 95%), tetraethyl orthosilicate (TEOS, 98%), sulfanilamide (99%), captopril (99%) and 5-Fluorouracil (5-Fu, 99%), acetonitrile, ethanol, HCl, phosphate buffer solution (PBS), and simulated body fluid (SBF) buffer were purchased from Aldrich, USA. All chemicals were used as received without any further purification. Water used in all syntheses was distilled and deionized.

2.2. Preparation of BSDU

Sulfanilamide (1.72 g, 10 mmol) was dissolved in 40 mL of dry acetonitrile. To this IPTES (4.62 g, 20 mmol), 10 mL of dry acetonitrile was added slowly under nitrogen atmosphere (Scheme 1). The mixture was refluxed for 24 h under inert condition. The reaction was monitored by TLC (thin layer chromatography) analysis. The solvent was evaporated, followed by the production of white precipitates, which were dispersed in dry hexane for 1 h. The swelled white product was filtered, washed with hexane, and dried under vacuum.

$[(EtO)_3Si(CH_2)_3NHCO]_2SO_2C_6H_4$, Yield: 99%; ^{1}H NMR (300 MHz, $CDCl_3$): δ 0.5 (t, 4H, SiCH_2), δ 1.1 (t, 18H, CH_3CH_2O), δ 1.5 (t, 4H, SiCH_2CH_2), δ 3.0 (q, 4H, CH_2NH), δ 3.3 (t, 8H, NHCH_2) δ 3.7 (q, 12H, CH_3CH_2O), δ 4.3 (t, 2H, CH_2NH, propylamine), δ 7.6–7.8 (q, 4H, $CH_{benzene}$). ^{13}C NMR (300 MHz, $CDCl_3$): δ 0.38 (CH_2Si), δ 7.3 (CH_3), δ 18.5 (CH_2), δ 23.5 (NCH_2), δ 58.0 (CH_2O), δ 136.0 (NH–$C_{benzene}$), δ 146.9 (SO_2–$C_{benzene}$), δ 116.9 and 127.0 ($C_{benzene}$), δ 155.8 (C=O). FT-IR (KBr): 3351 cm^{-1} (ν_{NH}), 2978 and 2885 cm^{-1} (ν_{CH}), 1681 cm^{-1} (ν_{CO}), 1552 cm^{-1} ($\nu_{NH-amide}$), 1401 cm^{-1} (ν_{NC}), 1242 cm^{-1} (ν_{SiC}), 1314, 1159 cm^{-1} ($\nu_{S=O}$).

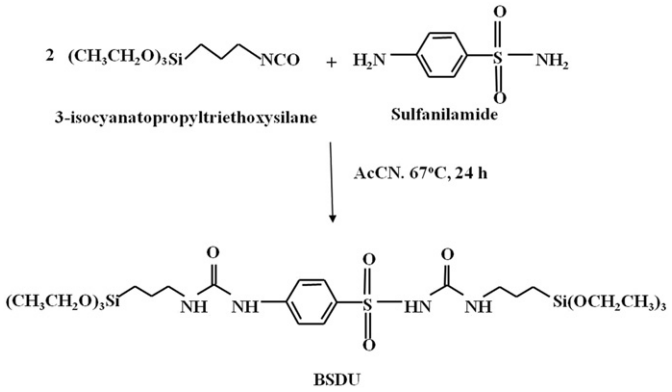

Scheme 1. Preparation of BSDU.

2.3. Synthesis of *N*,*N*′-diureylene-sulfanilamide bridged periodic mesoporous organosilicas (SDPMO)

N,*N*′-diureylenesulfanilamide bridged mesoporous materials were prepared using TEOS as the parent silica source, BSDU as the source of bridging organic groups and P123 as the structure-directing agent. A molar ratio of TEOS:BSDU:P123:HCl:H_2O=$(1-x)$:x:0.017:4.79:185, where x=0.025, 0.05, 0.075 and 0.10 has been used in the entire study. The materials synthesized were named as SDPMO-2.5, SDPMO-5, SDPMO-7.5 and SDPMO-10. In a typical procedure, a solution of P123, HCl and water was prepared at 35 °C. To this solution, a mixture of TEOS and BSDU were added slowly under vigorous stirring. The mixture was allowed to stir for 24 h at the above temperature after the formation of white precipitates, and further the heterogeneous mixture was aged for 24 h at 100 °C under stirring conditions. The white precipitates were recovered by filtration, washed with water and then dried at atmosphere. The surfactant template was removed from organosilica materials through solvent extraction from an HCl–ethanol solution. 1 g of the as-synthesized PMO materials were gently stirred for 24 h in a solution of HCl (36 wt%, 1.5 g) and 100 g ethanol at 60 °C. This procedure was repeated three times until the surfactants were totally removed. The powder was filtered, washed with ethanol, and dried at 60 °C overnight to obtain final material.

2.4. Drug adsorption and release

Captopril/5-Fluorouracil (5-Fu) were dissolved in water (10 mg/mL), and 0.1 g carrier material was added into 12 mL of the above solution. The mixture was then shaken for 24 h at room temperature, which was demonstrated to be long enough to reach the adsorption equilibrium. The porous materials incorporated with Captopril/5-Fu were collected by centrifugation, and washed with water, and then dried in an oven at 35 °C. The amount of drug loaded in the pores of the carrier was characterized quantitatively using a thermogravimetric analyzer (TGA). *In vitro* drug release experiments were carried out by placing the dried powder of carrier materials loaded with drug molecules placed into a dialysis membrane bag (molecular weight cutoff 5000 kDa), and then immersed into 40 mL of phosphate buffer solution (PBS).

Throughout our drug release study we have used the simulated body fluid (SBF) buffer solution having a physiological pH of 7.4 at 37 °C. The released concentration as a function of time was analyzed by UV–visible spectroscopy at 210/259 nm in SBF solution.

2.5. Characterization

Small-angle X-ray scattering (SAXS) measurements were performed using a synchrotron X-ray source of Pohang Accelerator Laboratory (PAL, Korea): Co-$K\alpha$ ($\lambda = 1.608$ Å) radiation with an energy range of 4–16 keV. Transmission electron microscopy (TEM) images were obtained with a JEOL 2010 electron microscope with an acceleration voltage of 200 kV. Scanning electron microscopy (SEM) images were recorded with a JEOL 6400 microscope operating at 20 kV. Fourier-transformed infra-red (FT-IR) spectra were obtained using a Perkin Elmer FT-IR spectrometer in the frequency range of 4000–400 cm^{-1}. The adsorption/desorption isotherms of nitrogen at −196 °C were measured using a Nova 4000e surface area and pore size analyzer. Before the measurement, the samples were degassed at 120 °C for 2 h in vacuo. The pore size distribution curve was obtained from an analysis of the adsorption branch using the Barrett–Joyner–Halenda (BJH) method. ^{13}C cross polarization (CP) and ^{29}Si MAS NMR spectra were obtained with a Bruker DSX400 spectrometer with a 4 mm zirconia rotor spinning at 6 kHz (resonance frequencies of 79.5 and 100.6 MHz for ^{29}Si and ^{13}C CPMAS NMR spectroscopy, respectively. A 90° pulse width of 5 μs, contact time 2 ms, recycle delay 3 s for both ^{29}Si MAS and ^{13}C CP MAS NMR spectroscopy have been utilized throughout the analysis). Thermogravimetric analysis (TGA) was performed with a Perkin–Elmer Pyris Diamond TG instrument at a heating rate of 10 °C min^{-1} in air.

3. Results and discussion

3.1. Small angle X-ray scattering analysis (SAXS)

Fig. 1 displays the SAXS patterns of the samples SDPMO-2.5, SDPMO-5, SDPMO-7.5 and SDPMO-10. All samples show three scattering peaks that can be indexed as 100, 110 and 200 reflections, respectively, associated with hexagonal arrays of mesopores [36], though a less intense scattering patterns were obtained with increasing the fraction of the bridged disiloxane precursor, indicating the weaker integrity of the two-dimensional (2D) hexagonal mesostructure. The 110 and 200 scattering peaks of the SDPMO-2.5, SDPMO-5 and SDPMO-7.5 were persisting, but for SDPMO-10 the above peaks were not resolved fully due to the partial structural demolish and the lack of long range order. The above observation suggests that the presence of the excessive complex organic building blocks inside the pore walls would decrease the mesoscopic order of the PMOs and lead to the collapse of the mesoporous structure.

3.2. TEM and SEM images

Representative TEM images of SDPMO-7.5 and SDPMO-10 shown in Fig. 2A provides excellent evidences for the periodic hexagonal arrangement of the PMOs after surfactant extraction, which is consistent with the SAXS patterns. The sample SDPMO-7.5 shows good long range order, confirming the 2D hexagonal mesostructure [37]. But the SDPMO-10 shows a disordered pore structure in the TEM image, which may be due to the partial destruction to the channels. The SEM images shown in Fig. 2B demonstrate a morphology transition trend of the PMOs with the increase of BSDU. For SDPMO-2.5, the morphology is somewhat irregular short rods, while going to higher loading of the disilane

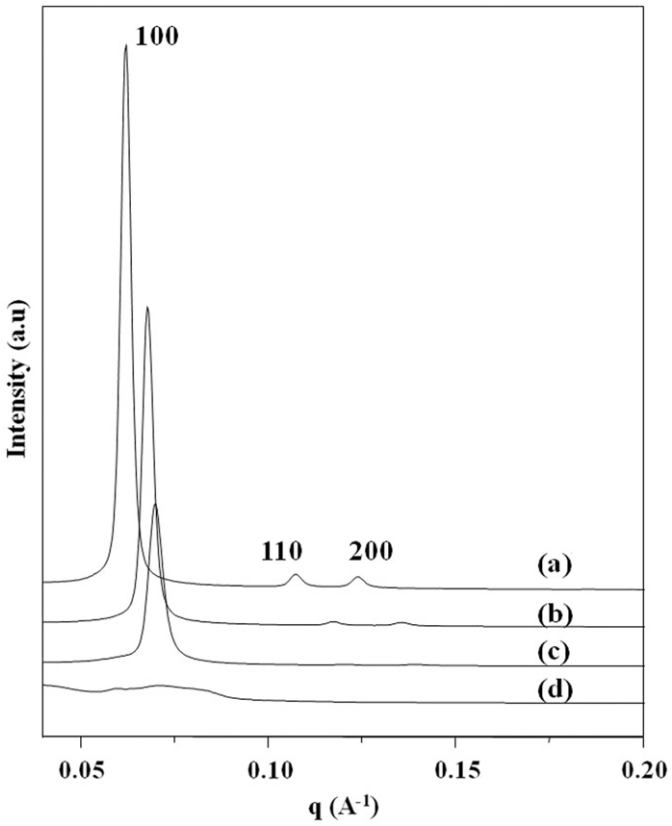

Fig. 1. Small angle X-ray scattering patterns of (a) SDPMO-2.5, (b) SDPMO-5, (c) SDPMO-7.5, and (d) SDPMO-10.

precursor there is an elongation and further aggregation has been observed. The rope like morphologies of SDPMO-7.5 and SDPMO-10 are the result of the electrostatic or hydrogen bonding interaction between the organosilane present in the materials. A deep inspection of SDPMO-7.5 and SDPMO-10 morphologies tells the fact that there is an increased tendency for side on packing due to the increase in hydrophilic urea and sulfanilamide functionalities in the materials. SDPMO-2.5 and SDPMO-5 show a particle length of 1.8 and 2.4 μm and a diameter of 0.6 and 1.6 μm, respectively. Due to the particle aggregation nature of the samples SDPMO-7.5 and SDPMO-10 was hard to clarify the exact particle length and diameter.

3.3. N_2-adsorption desorption study

Low temperature nitrogen adsorption–desorption isotherms for 2D hexagonal (*p6mm*) SDPMOs are shown in Fig. 3A. All isotherms displayed type IV patterns with steep capillary condensation/evaporation steps at P/P_0 of 0.65–0.80 and obvious H1 hysteresis loops, characteristic of mesoporous materials according to the IUPAC classification. The BET surface areas for this series of SDPMOs are in the range from 611 to 100 $m^2\,g^{-1}$, and the total pore volumes vary from 1.01 to 0.12 $cm^3\,g^{-1}$ (Table 1). As seen from Fig. 3A, and B, the sorption isotherm and the corresponding pore size distribution change gradually for the SDPMO samples from SDPMO-2.5 to SDPMO-10. The capillary condensation step shifts to lower P/P_0 values with increasing concentration of BSDU in the initial sol mixture, suggesting the gradual decreasing of the pore diameter from SDPMO-2.5 to SDPMO-10 and having a relative pressure range of $P/P_0 = 0.43–0.56$. This is expected because of the geometrical constrictions to accommodate a large number of lengthy BSDU bridging groups in the mesopore walls of the SDPMOs. The specific surface area of SDPMOs decreases from

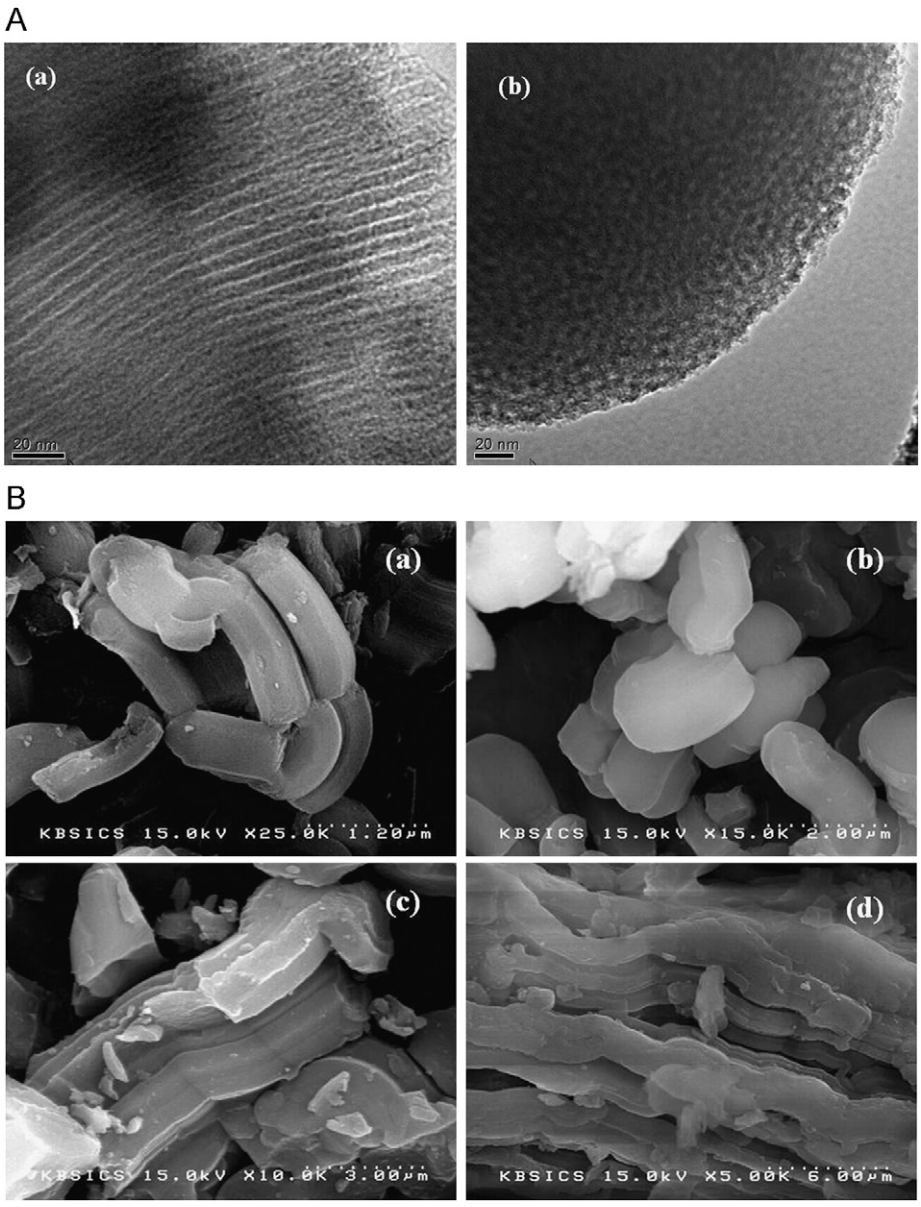

Fig. 2. (A) Transmission electron microscopic images of (a) SDPMO-7.5 and (b) SDPMO-10 and (B) Scanning electron microscopic images of (a) SDPMO-2.5, (b) SDPMO-5, (c) SDPMO-7.5 and (d) SDPMO-10.

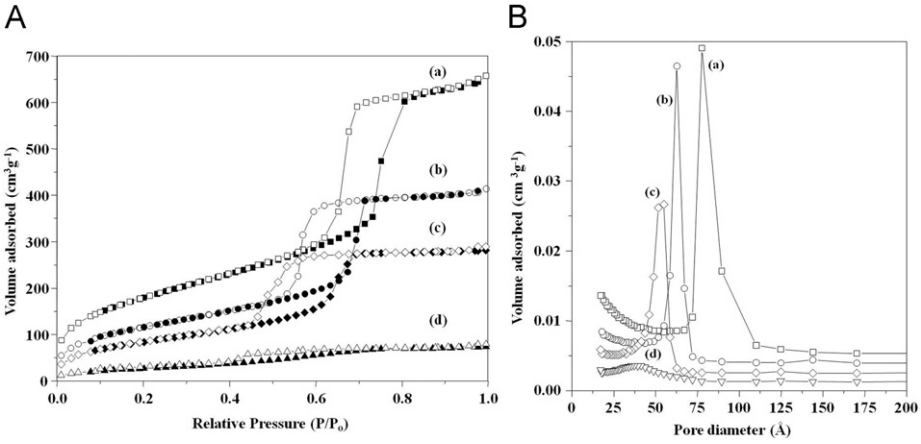

Fig. 3. (A) N_2 adsorption–desorption isotherms and (B) Pore size distributions of (a) SDPMO-2.5, (b) SDPMO-5, (c) SDPMO-7.5 and (d) SDPMO-10.

Table 1
Physico-chemical properties of diureylene–sulfonamide bridged mesoporous organosilica from N_2-sorption analysis.

Material	Specific surface area ($m^2\,g^{-1}$)	Pore diameter (Å)	Pore volume ($cm^3\,g^{-1}$)
SDPMO-2.5	611	61	1.01
SDPMO-5.0	403	59	0.63
SDPMO-7.0	311	56	0.44
SDPMO-10.0	100	48	0.12

663 to 100 $m^2\,g^{-1}$ with an enlargement of the diureylene–sulfanilamide moiety contents in the framework. It is worthy to mention that all SDPMO materials synthesized with different fractions of BSDU have ordered mesostructure with uniform pore size distributions. The pore diameter and pore volume of SDPMO-2.5, SDPMO-5, SDPMO-7.5 and SDPMO-10 were calculated to be 61, 59, 56 and 48 Å and 1.02, 0.63, 0.44 and 0.12 $cm^3\,g^{-1}$, respectively, decreasing with the fraction of BSDU. BSDU has a large molecular size and the bulk organic groups which can occupy more space of the mesopore walls in the case that a large amount of the guest is incorporated in the composite, resulting in a large reduction of the pore diameter and volume [1,38,39]. By increasing the BSDU fraction, more organic groups were incorporated into the silica matrix, leading to a SDPMO-10 with a broaden distribution of the pore size and a slightly distorted hexagonal mesostructure. The results are well consistent with the results of SAXS and TEM. Asefa et al. [38] reported that the surface area and pore volume did not decrease so much by increasing the loading amount of organic functional groups. Thus the sharply decrease of the surface area and pore volume with increasing the BSDU fraction may be caused by the damage of the mesostructure. However, the surface area or pore volume is strongly dependent on the type of organic moiety inside the PMO material. In the present study the organic molecule used is highly interactive and thus a regular packing would be possible in both walls and pores due to the presence of various functional groups therein. The plausible formation of hydrogen bonded interaction in this type of molecule may also cause a decrease in pore volume and surface area.

3.4. FTIR analysis

The FTIR spectra of solvent extracted SDPMO-*x* samples are shown in Fig. 4. In all the samples a broad and strong band at 3405 cm^{-1} can be due to N–H stretching vibration. The vibration bands at 2900–3000 cm^{-1} are assigned to the CH stretching vibrations of propyl and sulfanilamide moieties [1,4,5]. A sharp and intense band at 1646 cm^{-1} is attributed to the C=O stretching vibration of the urea group [40–43]. The bands at 1557 cm^{-1} together with 690 cm^{-1} result from the presence of the bending vibration of N–H, while the band at 1412 cm^{-1} is the characteristic of an N–C functional moiety inside the material [44]. The band from 1100–1000 cm^{-1} can be attributed to Si–O–Si stretching vibration, and the band at 670 cm^{-1} should be related with a bending vibration of O–Si–O bond. The results indicate the hydrolysis and co-condensation of the Si–OCH_2CH_3 groups. The intensity of 1700–1500 cm^{-1} bands increases gradually from the SDPMO-2.5 to the SDPMO-10 sample, which signifies the increased concentration of urea groups in the resultant materials. Moreover, a strong but broad band at 1250 cm^{-1} in all the samples for the vibration of Si–C indicates that the Si–C bond has not been broken during the synthesis process [45–47]. The weak bands at 2900–3000, 1348 and 1377 cm^{-1} not only implies the presence of C–H moieties but also the complete removal of P123 surfactant by ethanol extraction.

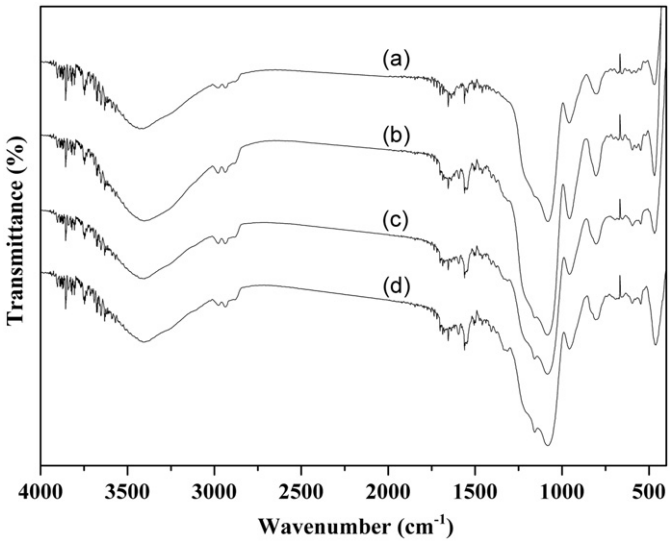

Fig. 4. FTIR spectra of (a) SDPMO-2.5, (b) SDPMO-5, (c) SDPMO-7.5 and (d) SDPMO-10.

3.5. Solid state ^{29}Si MAS and ^{13}C CP MAS NMR analysis

Solid-state ^{29}Si MAS NMR spectrum (Fig. 5a) of the surfactant-extracted SDPMO-7.5 material confirmed the successful incorporation of the covalently anchored organic groups in the framework. Two groups of signals can be distinguished in the spectrum: (a) three Q signals from silicon atoms without organic substitution and (b) two T signals related to organo-substituted silicon. The Q signals at −86, −94, and −101 ppm were assigned to Q^2, Q^3, and Q^4 structures, respectively. The Q^3 signal, corresponding to SiO_3OH, is clearly dominating, while the Q^4 signal caused by SiO_4 groups generated from fully condensed silanol groups. The Q^2 signal, related to partially condensed $SiO_2(OH)_2$, contributes with less percentage [48–50]. The signals originating from silicon bridged by the organic group can be found in the range from −45 to −90 ppm, thus confirming the incorporation of organic groups inside the framework [51]. The signals at −59 and −65 ppm can be assigned to the silicon resonances of partially condensed T^2 [$(SiO)_2(OH)SiC$] and fully condensed T^3 [$(SiO)_3SiC$] sites, respectively, indicating both the presence of organic moieties inside the framework and the high degree condensation of the silanol groups.

Fig. 5b exhibits the ^{13}C CP–MAS NMR spectrum of the SDPMO-7.5 sample after solvent extraction. Three signals (0–50 ppm) are observed, due to the Si–$CH_2CH_2CH_2$– groups, demonstrating the presence of the Si–C bond. The resonance at 10.5 ppm is attributed to –CH_2, which is directly bonded to a Si atom. The resonance at 17.6 ppm represents –CH_2, at 24.2 ppm for a –CH_2 carbon atom directly bonded to the –NH group, respectively. Furthermore, the resonance of C=O at 158.6 ppm can also be observed with a weak intensity in SDPMOs. The existence of the phenyl group is identified from the remaining signals in the spectrum, i.e., δ=61.1, 72.7 and 76.1 ppm. The clear resolution of the four carbons can be attributed to the homogeneous conformation of the organic groups in the pore walls [52].

3.6. SDPMOs as drug delivery system

Fig. 6 shows the *in vitro* release profile of captopril and 5-fluorouracil at 37 °C from the samples SDPMO-2.5 and SDPMO-7.5 into the simulated body fluid (SBF) at pH=7.4. Captopril/5-fluorouracil has been introduced in both materials (SDPMO-2.5 and SDPMO-7.5), in order to study the influence of organosilica loading, pore size and particle morphology in drug

release. The quantities of captopril/5-fluorouracil adsorbed were measured by UV–vis spectroscopy and TG analysis {Fig. 7(A) and (B)}, which revealed amounts of 6.23 and 9.72 wt% in the case of captopril and 12.23 and 13.71 wt% in the case of 5-fluorouracil for SDPMO-2.5 and SDPMO-7.5, respectively. For comparison, the TG curves for SDPMO-7.5 without loading any drug are illustrated in Fig. 7 to show the removal of organic moieties due to the presence of organosilane in the material as a representative SDPMO, though the SDPMO materials synthesized with different molar ratio of BSDU/TEOS may show different weight loss. Upon heating under air, the SDPMO-7.5 without drug loading undergoes a total weight loss of 21%. The initial weight loss, until 393 K, was attributed to thermal desorption of water and another weight loss in the range of 393–506 K indicates the removal organic moieties due to the presence of organosilane in the material. Presumably, the rather extended temperature range is caused by several chemical reactions (e.g. urea decomposition, sulfonyl decomposition, oxidation reactions, and "channel metamorphosis") via proton transfer from silanols to methylene groups [48,53]. Even after loading drugs, similar TG patterns were observed for the typical SDPMO-7.5 except the further weight losses due to the decomposition of the loaded drugs. It is noteworthy that for the small-pore material (SDPMO-7.5), the apparent weight of captopril/5-fluorouracil molecule packed inside is higher than the large pore sized material (SDPMO-2.5) even though the material having less surface area. These results suggest a solid relation between the amount of organosilane loading and nature of the drug molecule, besides the particle size, pore diameter and surface area of the host material.

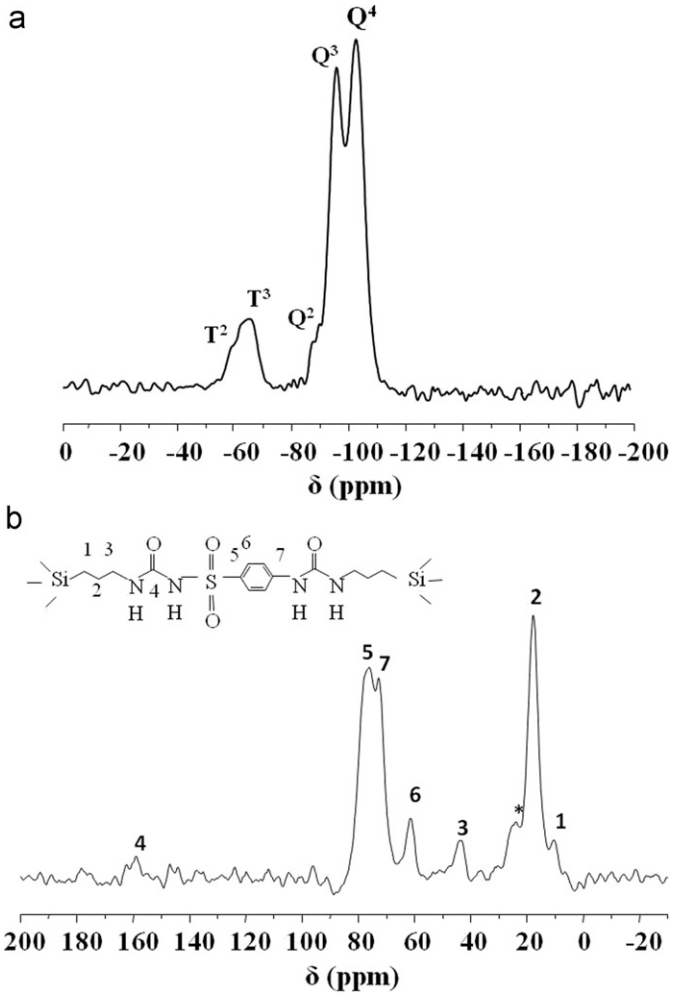

Fig. 5. (a) ^{29}Si MAS and (b) ^{13}C CP-MAS NMR spectra of SDPMO-7.5.

It has been shown elsewhere [54] that the driving force for the inclusion of captopril/5-fluorouracil inside the PMOs seems to be the hydrogen bond interaction between the captopril/5-fluorouracil molecule and the imine, sulfonyl or carbonyl functionality of the organo-bridged molecule in the pore wall. Moreover, 5-Fluorouracil having fluorine atom (exhibiting a strong hydrogen bonding) in the heterocyclic ring would create stronger hydrogen bonds with organo-bridged molecule in the pore wall than captopril and therefore results in the high drug loading. This is why the amount of 5-fluorouracil loading is higher than captopril for both PMOs under our experimental conditions.

It can be observed that all the release profiles are similar and exhibit sustained release bahaviors. The samples having pore diameters of 6.1 and 5.6 nm and block-and-rope like morphologies for SDPMO-2.5 and SDPMO-7.5, respectively. It was generally observed that increasing the pore size of the host material leads to a faster drug release rate and vice-versa. Therefore, in our study, a slower drug release rate has been observed while going from SDPMO-2.5 to SDPMO-7.5. The long mesoporous channel for the sample SDPMO-7.5 and higher % of BSDU organosilane are also favorable factors for the slower release of captopril/5-fluorouracil molecules [33,54]. The drug release process can be presumed to be mainly diffusion controlled. On the one hand, the release medium penetrates into the drug-matrix phase through pores; on the other hand, the drug dissolves into the release medium and diffuses from the system along with the solvent filled pore channels. This process is practically supported by the hydrophilic nature of the silica

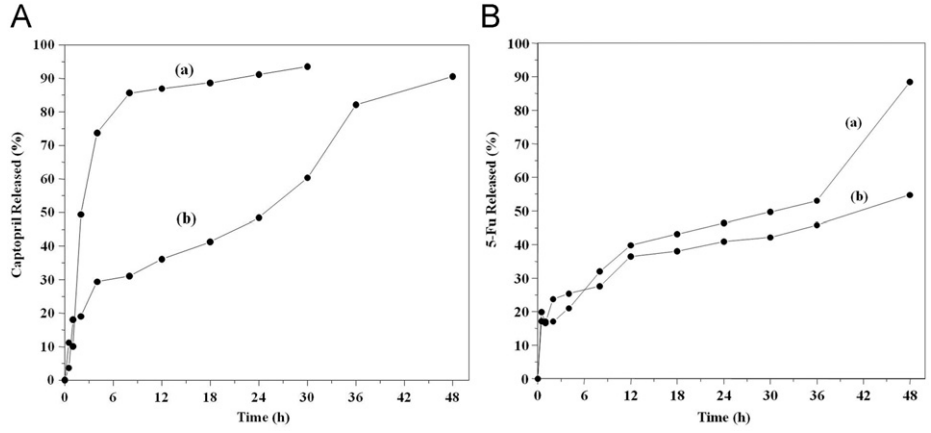

Fig. 6. (A) Captopril and (B) 5-Fluorouracil release profiles from (a) SDPMO-2.5 and (b) SDPMO-7.5.

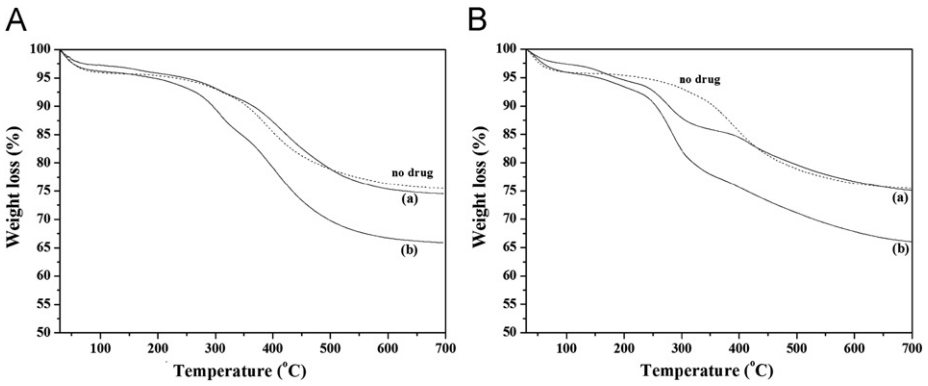

Fig. 7. TGA curves of (A) captopril and (B) 5-fluorouracil loaded (a) SDPMO-2.5 and (b) SDPMO-7.5. For comparison, TGA curves of SDPMO-7.5 without any drugs are also presented (dotted lines denoted as "no drug.").

surface and the diureylene bridge molecule in the pore wall of the PMOs. Additionally, a large difference in the initial drug release rate for both PMOs is observed. For instance, the captopril release occurred 43% within 4 h while only 26% of 5-fluorouracil was released from the sample SDPMO-2.5. After the initial release, a slower desorption was observed for captopril while a drastic release occurred for 5-fluorouracil. This may be due to the less interaction between 5-fluorouracil with diureylene molecules than with captopril. The drug release from the sample SDPMO-2.5 seems to be completed within 48 h, particularly for 5-fluorouracil no release had been observed after 36 h. The drug release profile from the sample SDPMO-7.5 is strictly in a controlled manner for both captopril and 5-fluorouracil. When comparing the initial desorption behavior of both the drugs, 18% of 5-fluorouracil was released while 28% of captopril was released within 4 h. After that, a reduced amount of drug release was observed for both the drugs, which may be due to many favorable factors such as particle size, pore diameter, a greater amount of organosilane loading, and longer channels of the SDPMO-7.5 than SDPMO-2.5. Therefore, it can be concluded that the drug release behavior from the host material is governed by the morphology, the amount of organo-bridged molecules, the pore diameter, etc. [30].

The nature of the drug molecule and its interaction with the host matrix also plays an important role in controlled release [30,39]. Captopril/5-fluorouracil drug chosen in the present study is that the first one (Captopril) is highly hydrophilic and the second one (5-Fu) is weakly hydrophilic. Nevertheless, 5-Fluorouracil would create stronger hydrogen bonding with the diureylene molecule due to the presence of fluorine atom in the heterocyclic ring of its molecular structure than captopril.

Meanwhile, SBA-15 is another important mesoporous material with large, controlled pore size and highly ordered hexagonal topology. The pore size of SBA-15 is usually large. Therefore, SBA-15 is expected to have less restriction for the delivery of bulky molecules compared to SDPMOs. However, for pure SBA-15, there exist only silanol groups on the channel walls, and these silanol groups simply form weak intermolecular hydrogen bonds with drugs, hence, they are not strong enough to hold drugs and allow them to be released in a sustained manner [55]. Therefore, introduction of functional groups on the surface of SBA-15 to have specific host–guest interactions with drugs will also be important and desirable for controlled drug delivery [56].

4. Conclusions

New diurea sulfanilamide bridged mesoporous organosilicas have been successfully synthesized by an one step co-condensation of TEOS and BSDU precursors in presence of Pluronic P123 as a template. The as-prepared SDPMO samples conserve regular rope-like morphology, and exhibit mesoporous structure, which is suitable for controlled release as a drug carrier. The combination of several characterization techniques have demonstrated that diurea sulfanilamide bridged molecule has been successfully incorporated in the wall of the PMO materials. Also it was confirmed that a maximum amount of organic groups incorporated into the PMOs reached up to 10 mol% according to the total silane content. However the incorporation of the complex organic group would slightly decrease the macroscopic order. Anyway, the drug release process from the matrix into a simulated body fluid (SBF) solution showed that the diurea sulfanilamide modified PMO materials are well controlled due to the presence of hydrophilic ureylene moieties, which supports the potential use of the materials as suitable controlled drug delivery carriers at a pH 7.4.

Acknowledgments

This work was supported by the Ministry of Education, Science and Technology (MEST) through the National Research Foundation of Korea (NRF) with the Acceleration Research Program (No. 2010 0000790), the Pioneer Research Center Program (2010-0019308/2010-0019482), and the Brain Korea 21 Project of the MEST.

References

[1] T. Asefa, M.J. MacLachlan, N. Coombs, G.A. Ozin, Nature 402 (1999) 867.
[2] S. Inagaki, S. Guan, Y. Fukushima, T. Ohsuna, O. Terasaki, J. Am. Chem. Soc. 121 (1999) 9611.
[3] B.J. Melde, B.T. Holland, C.F. Blanford, A. Stein, Chem. Mater. 11 (1999) 3302.
[4] M. Shakeri, K. Kawakami, Catal. Commun. 10 (2008) 165.
[5] H. Huang, C. Yang, H. Zhang, M. Liu, Micropor. Mesopor. Mater. 111 (2008) 254.
[6] A. Katiyar, L. Ji, P. Smirnitotis, N.G. Pinto, J. Chromatogr. A 1069 (2005) 119.
[7] S. Yuan, L. Shi, K. Mori, H. Yamashita, Micropor. Mesopor. Mater. 117 (2009) 356.
[8] Y. Liang, R. Anwwander, J. Mater. Chem. 17 (2007) 2506.
[9] G. Winzenburg, C. Schmidt, S. Fuchs, T. Kissel, Adv. Drug Deliv. Rev. 56 (2004) 1453.
[10] F. Ye, H. Guo, H. Zhang, X. He, Acta Biomater. 6 (2010) 2212.
[11] M.P. Ginebra, T. Traykova, J.A. Planell, J. Contro. Release 113 (2006) 102.
[12] I.I. Slowing, J.L. Vivero-Escoto, C.W. Wu, V.S.-Y. Lin, Adv. Drug Deliv. Rev. 60 (2008) 1278.
[13] D. Halamová, M. Badaničová, V. Zeleňák, T. Gondová, U. Vainio, Appl. Surf. Sci. 256 (2010) 6489.
[14] A. Sousa, K.C. Souza, E.M.B. Sousa, Acta Biomater. 4 (2008) 671.
[15] Q. Tang, Y. Xu, D. Wu, Y. Sun, J. Solid State Chem. 179 (2006) 1513.
[16] M. Benitez, D. Das, R. Ferreira, U. Pischel, H. Garcıa, Chem. Mater. 18 (2006) 5597.
[17] S. Angelos, M. Liong, E. Choi, J.I. Zink, Chem. Eng. J. 137 (2008) 4.
[18] Y.K. Seo, S.B. Park, D.H. Park, J. Solid State Chem. 179 (2006) 1285.
[19] Y. Luo, P. Yang, J. Lin, Micropor. Mesopor. Mater. 111 (2008) 194.

[20] L. Gao, F. Wei, Y. Zhou, X.X. Fan, Y. Wang, J.H. Zhu, Chem. Asian J. 4 (2009) 587.
[21] J. Li, T. Qi, L. Wang, Y. Zhou, C. Liu, Y. Zhang, Micropor. Mesopor. Mater. 103 (2007) 184.
[22] G. Cavallaro, P. Pierro, F.S. Palumbo, F. Testa, L. Pasqua, R. Aiello, Drug Deliv. Rev. 11 (2004) 41.
[23] M.V. Regi, A. Ramila, R.P. Del Real, J.P. Pariente, Chem. Mater. 13 (2001) 308.
[24] P.X. Zhi, H.Z. Qing, Q.L. Gao, B.Y. Ai, Chem. Eng. Sci. 61 (2006) 1027.
[25] M.V. Regi, Chem. Eur. J. 12 (2006) 5934.
[26] M. Hartmann, Chem. Mater. 17 (2005) 4577.
[27] H.H.P. Yiu, P.A. Wright, J. Mater. Chem. 15 (2005) 3690.
[28] M.S. Papkov, K. Agashi, A. Olaye, K. Shakesheff, A.J. Domb, Adv. Drug Deliv. Rev. 59 (2007) 187.
[29] C. Barbe, J. Bartlett, L.G. Kong, K. Finnie, H.Q. Lin, M. Larkin, S. Calleja, A. Bush, G. Calleja, Adv. Mater. 16 (2004) 1959.
[30] M.V. Regı, F. Balas, D. Arcos, Angew. Chem. Int. Ed. 46 (2007) 7548.
[31] R. Mellaerts, C.A. Aerts, J.V. Humbeeck, P. Augustijns, G.V. Mooter, J.A. Martens, Chem. Commun. 13 (2007) 1375.
[32] F. Qu, G. Zhu, S. Huang, S. Li, J. Sun, D. Zhang, S. Qiu, Micropor. Mesopor. Mater. 92 (2006) 1.
[33] F.Y. Qu, G.S. Zhu, S.Y. Huang, S.G. Li, S.L. Qiu, Chem. Phys. Chem. 7 (2006) 400.
[34] S.J. Son, J. Reichel, B. He, M. Schuchman, S.B. Lee, J. Am. Chem. Soc. 127 (2005) 7316.
[35] C. Li, J. Yang, X. Shi, J. Liu, Q. Yang, Micropor. Mesopor. Mater. 98 (2007) 220.
[36] D. Jiang, J. Gao, Q. Yang, J. Yang, C. Li, Chem. Mater. 18 (2006) 6012.
[37] M.A. Wahab, I. Imae, Y. Kawakami, C.S. Ha, Chem. Mater. 17 (2005) 2165.
[38] T. Asefa, M. Kruk, M.J. MacLachlan, N. Coombs, H. Grondey, M. Jaroniec, G.A. Ozin, J. Am. Chem. Soc. 123 (2001) 8520.
[39] T. Asefa, M. Kruk, M.J. MacLachlan, N. Coombs, H. Grondey, M. Jaroniec, G.A. Ozin, Adv. Funct. Mater. 11 (2001) 447.
[40] J.J.E. Moreau, L. Vellutini, M.W.C. Man, C. Bied, J. Am. Chem. Soc. 123 (2001) 1509.
[41] J.J.E. Moreau, L. Vellutini, M.W.C. Man, C. Bied, Chem. Eur. J. 9 (2003) 1594–1599.
[42] J.J.E. Moreau, L. Vellutini, M.W.C. Man, C. Bied, J.L. Bantignies, P. Dieudonne, J.L. Sauvajol, J. Am. Chem. Soc. 123 (2001) 7957.
[43] J.J.E. Moreau, B.P. Pichon, M.W.C. Man, C. Bied, H. Pritzkow, J.L. Bantignies, P. Diudonne, J.L. Sauvajol, Angew. Chem. Int. Ed. 43 (2004) 203.
[44] C. Franville, D. Zambon, R. Mahiou, Y. Troin, Chem. Mater. 12 (2000) 428.
[45] O. Muth, C. Schellbach, M. Froba, Chem. Commun. 19 (2001) 2032.
[46] D. Zhao, J. Feng, Q. Huo, N. Melosh, G.H. Fredrickson, B.F. Chmelka, G.D. Stucky, Science 279 (1998) 548.
[47] M.A. Wahab, W. Guo, W.J. Cho, C.S. Ha, J. Sol–Gel Sci. Technol. 27 (2003) 333.
[48] W.P. Guo, J.Y. Park, M.O. Oh, H.W. Jeong, W.J. Cho, I. Kim, C.S. Ha, Chem. Mater. 15 (2003) 2295.
[49] Ö. Dag, C.Y. Ishii, T. Asefa, M. MacLachlan, H. Grondey, N. Coombs, G.A. Ozin, Adv. Funct. Mater. 11 (2001) 213.
[50] W. Whitnall, T. Asefa, G.A. Ozin, Adv. Funct. Mater. 15 (2005) 1696.
[51] S. Huh, J.W. Wiench, J.C. Yoo, M. Pruski, V.S.Y. Lin, Chem. Mater. 15 (2003) 4247.
[52] O. Olkhovyk, S. Pikus, M. Jaroniec, J. Mater. Chem. 15 (2005) 1517.
[53] A. Rámila, B. Munoz, J.P. Pariente, M.V. Regí, J. Sol–Gel Sci. Technol. 26 (2003) 1199.
[54] J. Andersson, J. Rosenholm, S. Areva, M. Linden, Chem. Mater. 16 (2004) 4160.
[55] S. Wang, Micropor. Mesopor. Mater. 117 (2009) 1.
[56] Q. Yang, S. Wang, P. Fan, L. Wang, Y. Di, K. Lin, F.-S. Xiao, Chem. Mater. 17 (2005) 5999.